iScience

CellPress
OPEN ACCESS

Article

Real-time three-dimensional tracking of single vesicles reveals abnormal motion and pools of synaptic vesicles in neurons of Huntington's disease mice

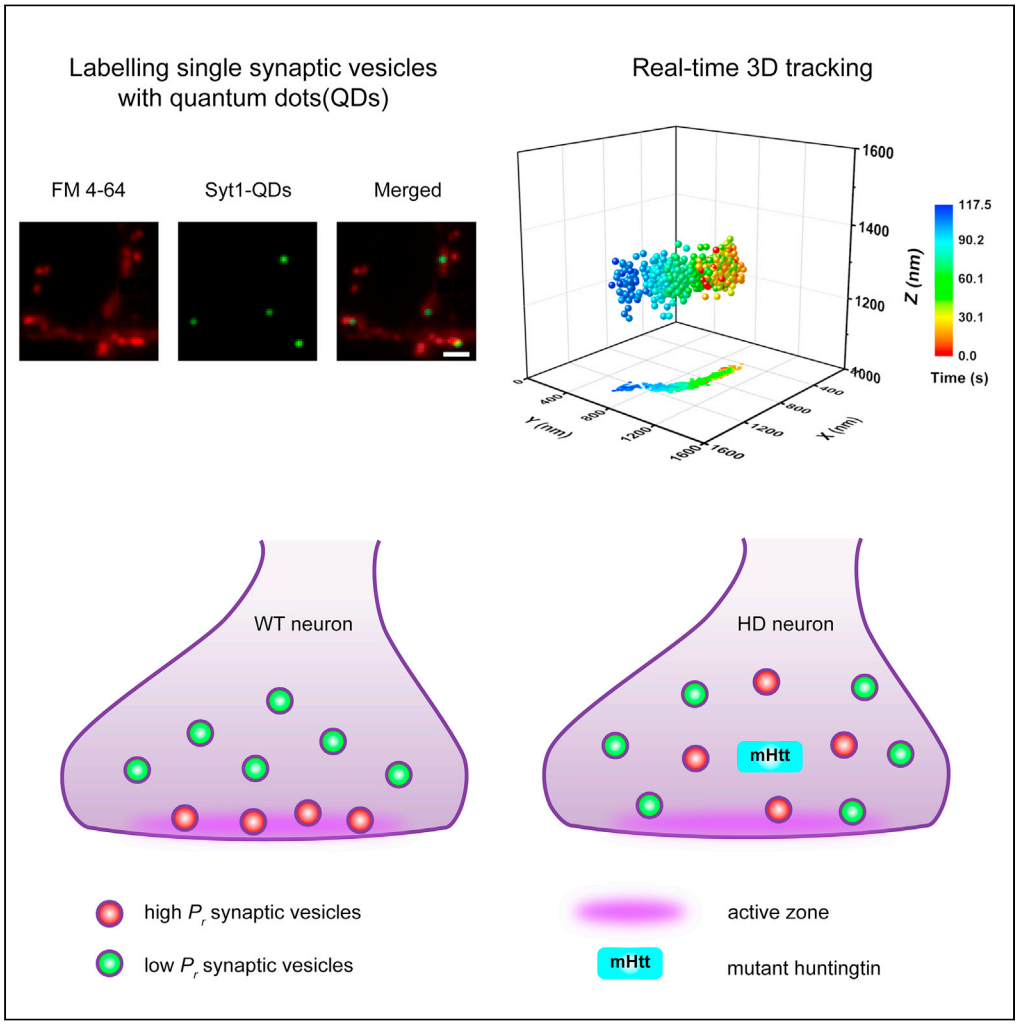

Sidong Chen, Hanna Yoo, Chun Hei Li, ..., Li Yang Tan, Sangyong Jung, Hyokeun Park

hkpark@ust.hk

Highlights

Real-time 3D tracking of single synaptic vesicles in living neurons was performed

3D tracking revealed abnormal motion and pools of releasing vesicles in HD neurons

Non-releasing vesicles in HD neurons showed prevalent irregular oscillatory motion

These abnormalities in HD can be rescued by Rab11 and jasplakinolide respectively

Chen et al., iScience 24, 103181
October 22, 2021
https://doi.org/10.1016/j.isci.2021.103181

iScience

CellPress
OPEN ACCESS

Article

Real-time three-dimensional tracking of single vesicles reveals abnormal motion and pools of synaptic vesicles in neurons of Huntington's disease mice

Sidong Chen,[1] Hanna Yoo,[1] Chun Hei Li,[1] Chungwon Park,[1] Gyunam Park,[2,3] Li Yang Tan,[4,5] Sangyong Jung,[4,6] and Hyokeun Park[1,7,8,9,*]

SUMMARY

Although defective synaptic transmission was suggested to play a role in neurodegenerative diseases, the dynamics and vesicle pools of synaptic vesicles during neurodegeneration remain elusive. Here, we performed real-time three-dimensional tracking of single synaptic vesicles in cortical neurons from a mouse model of Huntington's disease (HD). Vesicles in HD neurons had a larger net displacement and radius of gyration compared with wild-type neurons. Vesicles with high release probability (P_r) were interspersed with low-P_r vesicles in HD neurons, whereas high-P_r vesicles were closer to fusion sites than low-P_r in wild-type neurons. Non-releasing vesicles in HD neurons had an abnormally high prevalence of irregular oscillatory motion. These abnormal dynamics and vesicle pools were rescued by overexpressing Rab11, and the abnormal irregular oscillatory motion was rescued by jasplakinolide. Our studies reveal the abnormal dynamics and pools of synaptic vesicles in the early stages of HD, suggesting a possible pathogenic mechanism of neurodegenerative diseases.

INTRODUCTION

Neuronal communication is mediated by the efficient, precise, and tightly regulated release of neurotransmitters from synaptic vesicles in presynaptic terminals (Sudhof and Rizo, 2011); thus, alteration in the properties of synaptic vesicles can have effects on basal synaptic transmission (Alabi and Tsien, 2012), as well as short-term and long-term synaptic plasticity (Liu, 2003). A large body of evidence has demonstrated the general physiological and morphological properties of synaptic vesicles (Jahn and Fasshauer, 2012; Tao et al., 2018). Although two-dimensional tracking provided useful information about the motion of vesicles (Forte et al., 2017; Kamin et al., 2010; Lee et al., 2012; Peng et al., 2012; Westphal et al., 2008), the precise investigation of single synaptic vesicles in real time before, during, and after exocytosis (i.e., fusion) has remained challenging because of both technical and practical limitations. These limitations include the complexity associated with the three-dimensional structure of presynaptic terminals and the minuscule size of synaptic vesicles, which have an average diameter of approximately 40 nm, well below the resolution of conventional light microscopy (Yu et al., 2016). Recently, we developed a method for tracking the three-dimensional positions of single synaptic vesicles in real time in cultured hippocampal neurons using quantum dots (QDs) and dual-focus imaging optics, providing localization with an accuracy on the order of tens of nanometers (Park et al., 2012). In addition, we used this approach to examine the relationship between a single synaptic vesicle's location and its release probability (P_r) (Park et al., 2012). Although alteration in synaptic vesicle dynamics may play a pathogenic role in the early stages of neurodegenerative diseases such as Alzheimer's (Zhou et al., 2017), Parkinson's (Kyung et al., 2018), and Huntington's disease (HD) (Chen et al., 2018), the precise mechanisms that underlie these changes remain largely unknown, due in large part to the relative paucity of studies regarding the motion and release properties of single synaptic vesicles in the context of neurodegeneration.

Huntington's disease (HD) is a neurodegenerative disorder caused by an increase in CAG repeats in the huntingtin (*HTT*) gene and a corresponding expansion of the polyglutamine (polyQ) tract in the N-terminus of the huntingtin protein (MacDonald et al., 1993). Although the huntingtin protein is expressed throughout the body, medium spiny neurons in the striatum and pyramidal neurons in the cortex are particularly vulnerable to the polyQ expansion in the huntingtin protein (Vonsattel and DiFiglia, 1998). Under physiological

[1]Division of Life Science, The Hong Kong University of Science and Technology, Clear Water Bay, Kowloon, Hong Kong

[2]Creative Research Initiative Center for Chemical Dynamics in Living Cells, Chung-Ang University, Seoul 06974, South Korea

[3]Department of Chemistry, Chung-Ang University, Seoul 06974, South Korea

[4]Institute of Molecular and Cell Biology (IMCB), Agency for Science Technology and Research (A*STAR), Singapore

[5]Department of Psychological Medicine, Yong Loo Lin School of Medicine, National University of Singapore, Singapore 119077, Singapore

[6]Department of Physiology, Yong Loo Lin School of Medicine, National University of Singapore, Singapore 119077, Singapore

[7]Department of Physics, The Hong Kong University of Science and Technology, Clear Water Bay, Kowloon, Hong Kong

[8]State Key Laboratory of Molecular Neuroscience, The Hong Kong University of Science and Technology, Clear Water Bay, Kowloon, Hong Kong

[9]Lead contact

*Correspondence: hkpark@ust.hk

https://doi.org/10.1016/j.isci.2021.103181

conditions, the huntingtin protein is involved in a variety of cellular functions, including the transport of vesicles and organelles (Saudou and Humbert, 2016; Schulte and Littleton, 2011; Yu et al., 2018), transcriptional regulation (Benn et al., 2008; Saudou and Humbert, 2016; Schulte and Littleton, 2011), and cell survival (Ho et al., 2001; Rigamonti et al., 2001). It is therefore reasonable to speculate that the mutant huntingtin protein with an expanded polyglutamine repeat may disrupt these functions, leading to neuronal death in the striatum and cortex of HD patients. Interestingly, the mutant huntingtin protein has been shown to alter the release of neurotransmitters from synaptic vesicles (Cepeda and Levine, 2020; Chen et al., 2018; Joshi et al., 2009; Romero et al., 2008), contributing to the early onset of synaptic dysfunction in the preclinical stages of HD (Milnerwood and Raymond, 2010; Schippling et al., 2009), although the underlying mechanisms are not clearly understood.

Here, we tracked the real-time three-dimensional positions of single synaptic vesicles in cortical neurons cultured from an established HD knock-in mouse model and found the abnormal dynamics of single synaptic vesicles in HD neurons. Moreover, synaptic vesicles with high release probability (P_r) were interspersed with low-P_r vesicles in HD neurons. Besides, non-releasing synaptic vesicles in HD cortical neurons have an abnormally high prevalence of irregular oscillatory motion. The abnormal dynamics and vesicle pools of releasing synaptic vesicles in HD neurons were rescued by overexpressing Rab11 and the abnormal dynamics of non-releasing vesicles were rescued by stabilizing actin filaments with jasplakinolide. Taken together, we have provided the first observation of the abnormal dynamics and vesicle pools of single synaptic vesicles in the early stages of HD.

RESULTS

Abnormal motion of synaptic vesicles in HD neurons

First, we examined the motion and release of single synaptic vesicles which were loaded with a single streptavidin-coated quantum dot (QD) conjugated to commercially available biotinylated antibodies against the luminal domain of the vesicular protein synaptotagmin-1 (Syt1) (QD-loaded synaptic vesicles) (Figure 1A). For these experiments, we used primary cortical neurons cultured from wild-type (WT) mice and heterozygous zQ175 knock-in mice (HD) expressing the human *HTT* exon 1 sequence containing approximately 190 CAG repeats (Menalled et al., 2012); previous studies showed that these mice are a suitable mouse model for studying neurodegeneration in HD patients, particularly with respect to the underlying genetic defect and the disease's relatively late onset, slow progression, and neuropathology (Menalled et al., 2012).

Exocytosis of single QD-loaded synaptic vesicles during electrical stimulation was reflected by a rapid and irreversible drop in QD fluorescence intensity because of quenching by trypan blue (TB) in the extracellular solution (Figure 1B). Using this loading and quenching protocol, we can track the positions of single synaptic vesicles up until the moment of exocytosis (Park et al., 2012, 2021). The position of each QD-loaded synaptic vesicle in the *x-y* plane was determined to an accuracy on the order of tens of nanometers using FIONA (fluorescence imaging with one-nanometer accuracy) (Park et al., 2007; Yildiz and Selvin, 2005), and the position along the *z* axis was also determined to an accuracy on the order of tens of nanometers using dual-focusing imaging optics (Park et al., 2012, 2021; Watanabe et al., 2007), providing highly accurate three-dimensional trajectories in real time. To confirm the loading of synaptic vesicles in presynaptic terminals with QDs conjugated to biotinylated antibodies against synaptotagmin-1, we used FM4–64 to label spontaneously released synaptic vesicles and observed colocalization between the QD and FM4–64 fluorescence signals (Figures 1C and 1D). The similar loading efficiency of synaptic vesicles with QDs relative to one FM4–64 labeled presynaptic terminal (19.1 $\pm$ 1.07% (N = 10 experiments) for HD neurons vs. 19.3 $\pm$ 1.00% (N = 10) for WT neurons; p = 0.91, independent Student's *t*-test) (Figure S1) indicates that QDs conjugated to antibodies against the luminal domain of Syt1 were loaded inside synaptic vesicles in FM4–64 labeled presynaptic terminals in neurons regardless of genotypes.

Fluorescence images of the QD-loaded synaptic vesicles just before and after exocytosis regardless of genotypes show near-complete and irreversible quenching of QD fluorescence (Figures 1E and 1F), indicating exocytosis of QD-loaded synaptic vesicles. The release percentage of these single QDs-loaded synaptic vesicles during electrical stimulation was not altered by genotypes (52.1 $\pm$ 1.36% (N = 14 experiments) for HD neurons vs. 49.9 $\pm$ 2.33% (N = 14) for WT neurons; p = 0.42, independent Student's *t*-test) (Figure S2). In addition to the three-dimensional positions of QD-loaded synaptic vesicles, we analyzed the radial distance (*R*) from the momentary position to the fusion site (calculated using the

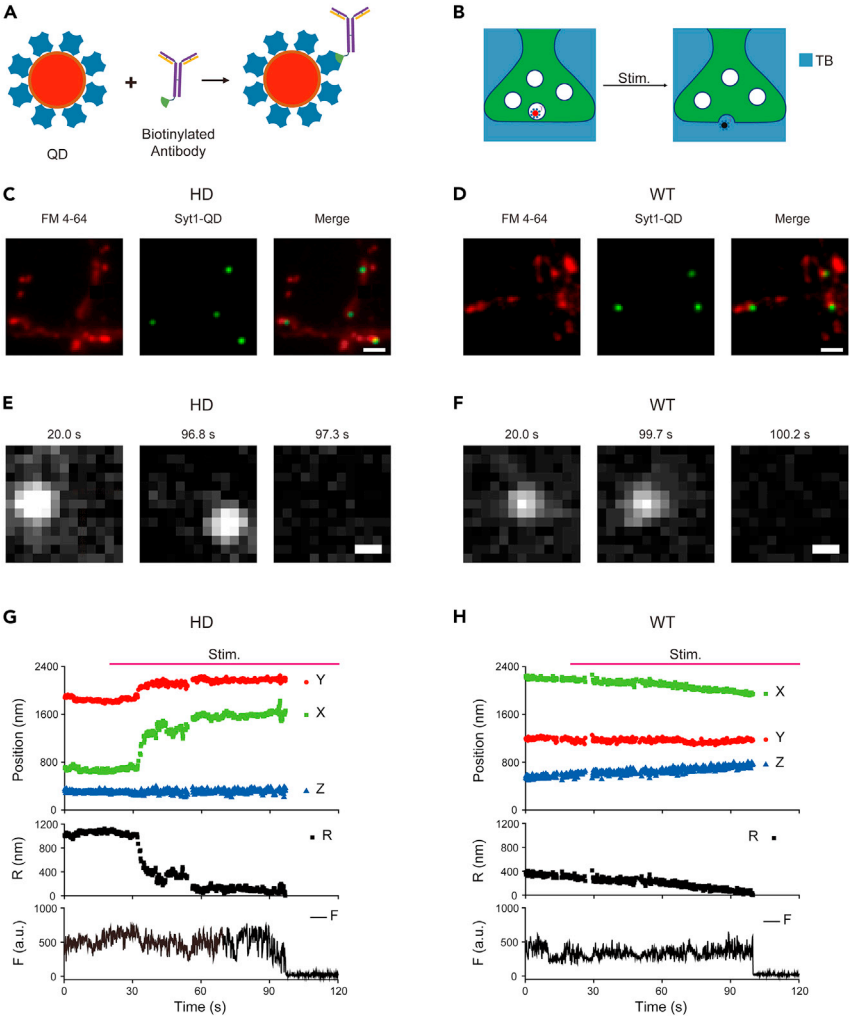

Figure 1. Real-time three-dimensional tracking of a single synaptic vesicle loaded with a single quantum dot (QD) in the presynaptic terminals of HD and WT cortical neurons

(A) Schematic diagram depicting a conjugation strategy. A biotinylated antibody against the luminal domain of synaptotagmin-1 (Syt1) was conjugated to a streptavidin-coated quantum dot (QD) for loading a synaptic vesicle with a single streptavidin-coated QD.

(B) Schematic diagram depicting a strategy to detect exocytosis of QD-loaded synaptic vesicles. After loading, extracellular trypan blue (TB) was used to quench the fluorescence of a QD in a synaptic vesicle undergoing exocytosis during stimulation, thereby indicating the moment of vesicle fusion.

(C and D) Colocalization of Syt1-QD–loaded synaptic vesicles (green) and FM4-64–labeled presynaptic terminals (red) in cultured HD (C) and WT cortical neurons (D). Observed colocalization between the QD and FM4–64 fluorescence signals indicates that QDs conjugated to antibodies against the luminal domain of Syt1 were loaded inside synaptic vesicles in the presynaptic terminals of neurons regardless of genotypes. Scale bar: 2 μm.

(E and F) Fluorescence images of the Syt1-QD–loaded vesicle taken at the indicated times in HD (E) and WT neurons (F). Fluorescence images of the QD-loaded synaptic vesicles just before (at 96.8 s in panel E and 99.7 s in panel F) and after exocytosis (at 97.3 s in panel E and 100.2 s in panel F) show near-complete and irreversible quenching of fluorescence regardless of genotypes, indicating exocytosis of QD-loaded synaptic vesicles. Scale bar: 0.5 μm.

(G and H) Representative time courses of the three-dimensional position, radial distance (R), and QD fluorescence (F) measured in the synaptic vesicles in panel E and F. Where indicated, neurons were stimulated at 10 Hz stimulation for 120 s. The three-dimensional radial distance was calculated from the momentary position to the fusion site ($R = \sqrt{\Delta X^2 + \Delta Y^2 + \Delta Z^2}$).

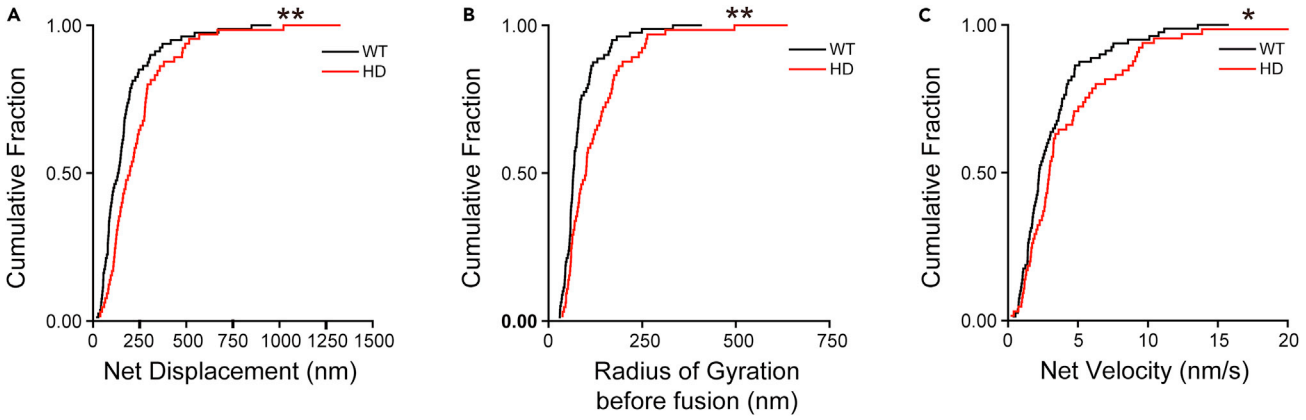

Figure 2. Synaptic vesicles in HD neurons have abnormal motion

(A–C) Cumulative plots for the net displacement (A), radius of gyration before fusion (B), and net velocity (C) of releasing synaptic vesicles in WT and HD neurons. The net displacement, radius of gyration before fusion, and velocity of releasing synaptic vesicles in HD (n = 65 vesicles, N = 14 experiments) neurons were significantly different from those in WT neurons (n = 80, N = 14). *p < 0.05, and **p < 0.01 (Kolmogorov–Smirnov (K-S) test).

equation $R = \sqrt{\Delta X^2 + \Delta Y^2 + \Delta Z^2}$, expressed in nm), and fluorescence intensity (F) in HD and WT neurons (Figures 1G and 1H). Fluorescence traces reveal a sharp and irreversible loss of fluorescence at around 97 s (Figure 1G) or 100 s (Figure 1H) caused by exposure of the QDs to trypan blue in the external solution, indicating exocytosis of QD-loaded synaptic vesicles. These traces illustrate that a single synaptic vesicle can be loaded with a single QD by endocytosis and can be successfully tracked in real time until exocytosis in three dimensions during electrical stimulation regardless of genotype. Interestingly, we found that the vesicle in the HD neuron was highly mobile prior to fusion (Figure 1G), whereas the vesicle in the WT neuron was relatively stationary (Figure 1H).

To study the dynamics of releasing synaptic vesicles, we calculated the net displacement between the initial positions in the beginning of imaging and the fusion sites of individual synaptic vesicles during electrical stimuli at 10 Hz. The three-dimensional net displacement of each vesicle was calculated as the Pythagorean displacement using our real-time three-dimensional traces of single QD-loaded synaptic vesicles. We found that the net displacement of synaptic vesicles in HD neurons was significantly larger compared with synaptic vesicles in WT neurons (242 $\pm$ 24.4 nm (average $\pm$ standard error of the mean (SEM)) (n = 65 vesicles, N = 14 experiments) vs. 170 $\pm$ 17.3 nm (n = 80, N = 14), respectively; p = 0.0049, Kolmogorov–Smirnov (K-S) test) (Figure 2A). We also estimated the volumetric space in which each synaptic vesicle traveled prior to exocytosis by calculating the three-dimensional radius of gyration (R_g) before fusion using the following equation (Qin et al., 2019):

$$R_g = \sqrt{\frac{1}{N}\sum_{i}^{N}[(x_i - \langle x\rangle)^2 + (y_i - \langle y\rangle)^2 + (z_i - \langle z\rangle)^2]}$$

in which N is the total number of time steps, x_i, y_i, and z_i are the projections in the x-, y-, and z-axes, respectively, at time step i, and $\langle x\rangle$, $\langle y\rangle$, and $\langle z\rangle$ are the average positions in each axis. As shown in Figure 2B, the radius of gyration before fusion of synaptic vesicles in HD neurons was significantly larger compared with WT neurons (125 $\pm$ 11.7 nm vs. 84 $\pm$ 6.5 nm, respectively; p = 0.0023, K-S test) (Figure 2B). Moreover, synaptic vesicles in HD neurons had higher velocity compared with WT neurons (4.8 $\pm$ 0.78 nm/s vs. 2.9 $\pm$ 0.25 nm/s, respectively; p = 0.033, K-S test) (Figure 2C). The dynamics of releasing synaptic vesicles in HD neurons before electrical stimulation was also significantly different from that in WT neurons (Figure S3). Taken together, these results indicate that synaptic vesicles in HD neurons are abnormal compared with WT neurons prior to exocytosis.

Abnormal vesicle pools of synaptic vesicles in HD neurons

We previously reported that the vesicle's release probability (P_r) is closely related to its synaptic location in rat hippocampal neurons; specifically, we found that synaptic vesicles close to their fusion sites have a higher P_r compared with vesicles located relatively far from their fusion sites (Park et al., 2012, 2021).

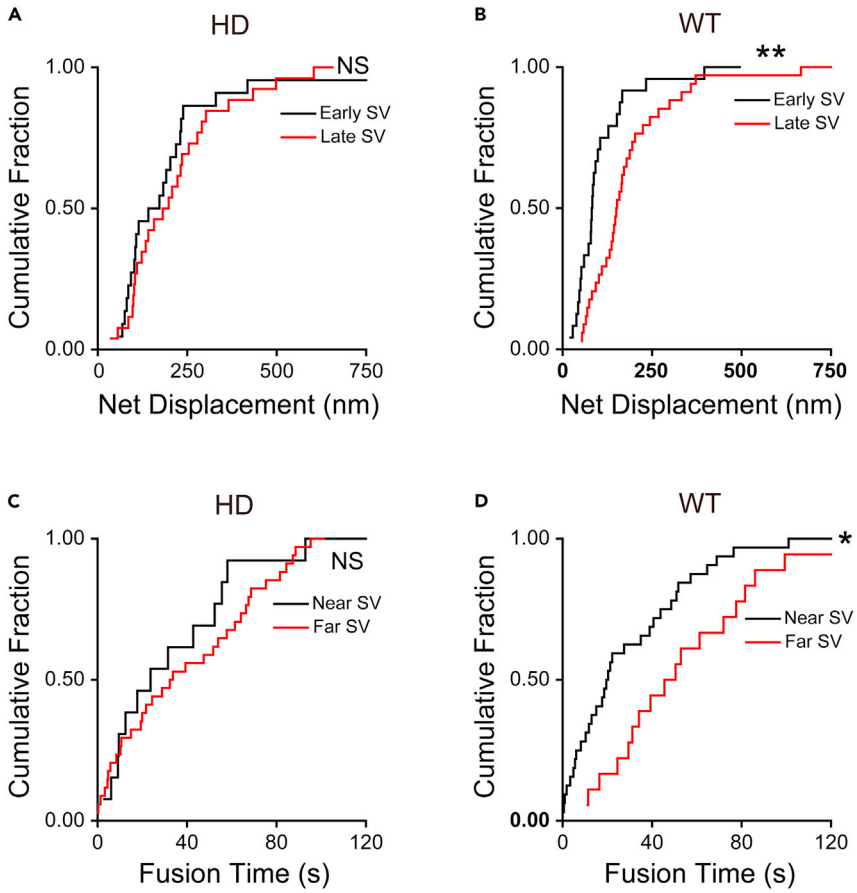

Figure 3. Synaptic vesicles in HD neurons have an abnormal relationship between release probability (P_r) and location

(A and B) Cumulative plots for the net displacement of early-releasing and late-releasing synaptic vesicles (defined as fusion time <20 s or >50 s, respectively, after the start of stimulation) in HD neurons (early SV, n = 22 vesicles; late SV, n = 26, N = 14 experiments) (A) and WT neurons (early SV, n = 24; late SV, n = 34, N = 14) (B).

(C and D) Cumulative plots for the fusion time between the onset of stimulation and fusion of synaptic vesicles initially located near or far from their fusion sites (defined as a net displacement <100 nm or >200 nm, respectively) in HD neurons (near SV, n = 13 vesicles; far SV, n = 34, N = 14 experiments) (C) and WT neurons (near SV, n = 32; far SV, n = 18, N = 14) (D). *p < 0.05, **p < 0.01, and NS, not significant (K-S test).

Thus, some synaptic vesicles located close to their fusion sites are docked to the presynaptic membrane and primed to rapidly release their contents upon Ca^{2+} influx.

To study this relationship in HD neurons, we analyzed fusion time of synaptic vesicles, which is defined as interval between the start of stimulation and fusion during electrical stimulation. Although the average fusion time of synaptic vesicles in HD neurons was smaller compared with WT neurons (39.9 ± 3.93 s (n = 65 vesicles) vs. 45.2 ± 3.83 s (n = 80), respectively) (Figure S4), the difference was not statistically significant (p = 0.87, K-S test). Considering the reported close relationship between the location of synaptic vesicles and release probability (Park et al., 2012, 2021), we defined high release probability (high P_r) as undergoing exocytosis within 20 s after the onset of stimulation (early SV) and low P_r as undergoing exocytosis after 50 s after the onset of stimulation (late SV). Synaptic vesicles with high P_r contain the readily releasable pool (RRP) and fast-releasing vesicles from the recycling pool (RP) (Alabi and Tsien, 2012). Consistent with previous findings, we found that synaptic vesicles with high P_r are located closer to their fusion sites compared with vesicles with low P_r in WT neurons (average net displacement, 111 ± 20.6 (n = 24 vesicles) nm vs. 192 ± 27.5 (n = 34) nm, respectively; p = 0.0026, K-S test)) (Figure 3B), which indicates that high-P_r and low-P_r vesicle pools were spatially separated in WT neurons. The plots of the net displacement between initial positions and fusion sites of all released synaptic vesicles against their fusion time are shown in Figure S5. In contrast, we found no difference in net displacement

between high-P_r vesicles and low-P_r vesicles in HD neurons (222 ± 53.6 nm (n = 22)) vs. 225 ± 29.7 (n = 26) nm, respectively; p = 0.88, K-S test)) (Figure 3A), indicating that high-P_r vesicles were interspersed with low-P_r vesicles in HD neurons. The relative portions of high-Pr and low-Pr synaptic vesicles in HD neurons were not significantly different from that in WT neurons (Figure S6). These results suggest an abnormal relationship between the vesicle's release probability and its location in HD neurons.

Next, we examined the relationship between the vesicle's initial location relative to its fusion site and fusion time in those neurons. In WT neurons, we found that synaptic vesicles initially located relatively near to their fusion sites (<100 nm (near SV)) had significantly shorter fusion time compared with synaptic vesicles initially located far away from their fusion sites (>200 nm (far SV)) (average fusion time, 30.2 ± 4.98 s (n = 32 vesicles) vs. 56.0 ± 8.06 s (n = 18), respectively; p = 0.030, K-S test) (Figure 3D); this finding is similar to our previous results obtained in rat hippocampal neurons (Park et al., 2012) and supports the close relationship between synaptic vesicle location and release probability. In contrast, we found no such difference in fusion time for synaptic vesicles located near and far from their fusion sites in HD neurons (36.6 ± 9.32 s (n = 13) vs. 40.7 ± 5.38 s (n = 34), respectively; p = 0.471, K-S test) (Figure 3C). Furthermore, correlation between net displacement and fusion time in WT neurons (Pearson's r = 0.563, Figure S5A) was stronger compared to HD neurons (Pearson's r = 0.366, Figure S5B). These results support an abnormal relationship between the vesicle's initial location and release probability in HD neurons.

Furthermore, we determined whether recycled synaptic vesicles from the readily releasable pool (RRP) are relocated back to close to their fusion sites following full-collapse fusion and retrieval from the presynaptic membrane. We tracked the location of the RRP vesicles loaded by applying 10 electrical stimuli at 10 Hz; for comparison, we also tracked the location of synaptic vesicles from the total recycling pool (TRP) labeled by applying 1200 electrical stimuli at 10 Hz. We found that in WT neurons, the recycled synaptic vesicles from the RRP were significantly closer to their fusion sites compared with recycled vesicles from the TRP (105 ± 8.0 nm (n = 28) vs. 170 ± 17.3 nm (n = 80) (p = 0.030, K-S test) (Figure S7A), similar to previous findings in rat hippocampal neurons (Park et al., 2012). In contrast, we found the no significant difference in net displacement between RRP and TRP recycled vesicles in HD neurons (253 ± 40.2 nm (n = 31) vs. 242 ± 24.4 nm (n = 65), respectively; p = 0.770, K-S test) (Figure S7B), suggesting that after fusion, RRP vesicles in HD neurons are not relocated close to their fusion sites. These results support the notion that synaptic vesicle pools are fundamentally abnormal in HD neurons.

Abnormal oscillatory motion of non-releasing synaptic vesicles in the presynaptic terminals of HD neurons

To further examine the abnormal motion of synaptic vesicles in the presynaptic terminals of HD neurons, we measured the motion of synaptic vesicles that failed to undergo fusion during the entire electrical stimulation period (i.e., non-releasing vesicles). Interestingly, we found that non-releasing synaptic vesicles in WT neurons generally showed directed (i.e., unidirectional) movement (Figure 4B); in contrast, non-releasing synaptic vesicles in HD neurons often displayed abnormal irregular oscillatory motion, which was characterized by moving back and forth (i.e., bidirectional) (Figure 4A). To quantify this motion, we defined irregular oscillatory motion as having a ratio between the radius of gyration and its net displacement >0.75; considering the size of the presynaptic terminal, we focused on vesicles with a net displacement <2 μm. We found that HD neurons contained an abnormally large percentage of non-releasing synaptic vesicles with irregular oscillatory motion compared with WT neurons (30.8 ± 3.96% (N = 14 experiments) vs. 10.0 ± 2.46% (N = 14), respectively; p = 0.0001, independent Student's *t*-test) (Figure 4C). Moreover, this abnormally high incidence of irregular oscillatory motion among non-releasing vesicles in HD neurons compared with non-releasing vesicles in WT neurons translated to a significantly larger travel distance (100 ± 7.0 μm (n = 47 vesicles) vs. 71 ± 4.4 μm (n = 43), respectively; p = 0.0006, K-S test) (Figure 4D), a significantly larger radius of gyration (216 ± 28.7 nm vs. 119 ± 13.3 nm, respectively; p = 0.0041, K-S test) (Figure 4E), and a significantly higher instantaneous speed compared with WT neurons (0.78 ± 0.053 μm/s vs. 0.57 ± 0.028 μm/s, respectively; p = 0.032, K-S test) (Figure 4F). Taken together, these results support the notion that non-releasing synaptic vesicles in HD neurons have abnormal motion within presynaptic terminals.

Overexpressing Rab11 rescues the abnormal dynamics and vesicle pools of releasing synaptic vesicles in HD neurons

The Ras-related small GTPase Rab11 is present on synaptic vesicles (Sudhof, 2004) and plays a role in vesicle recycling (Kokotos et al., 2018) and endosomal recycling (Ullrich et al., 1996). Moreover, Rab11

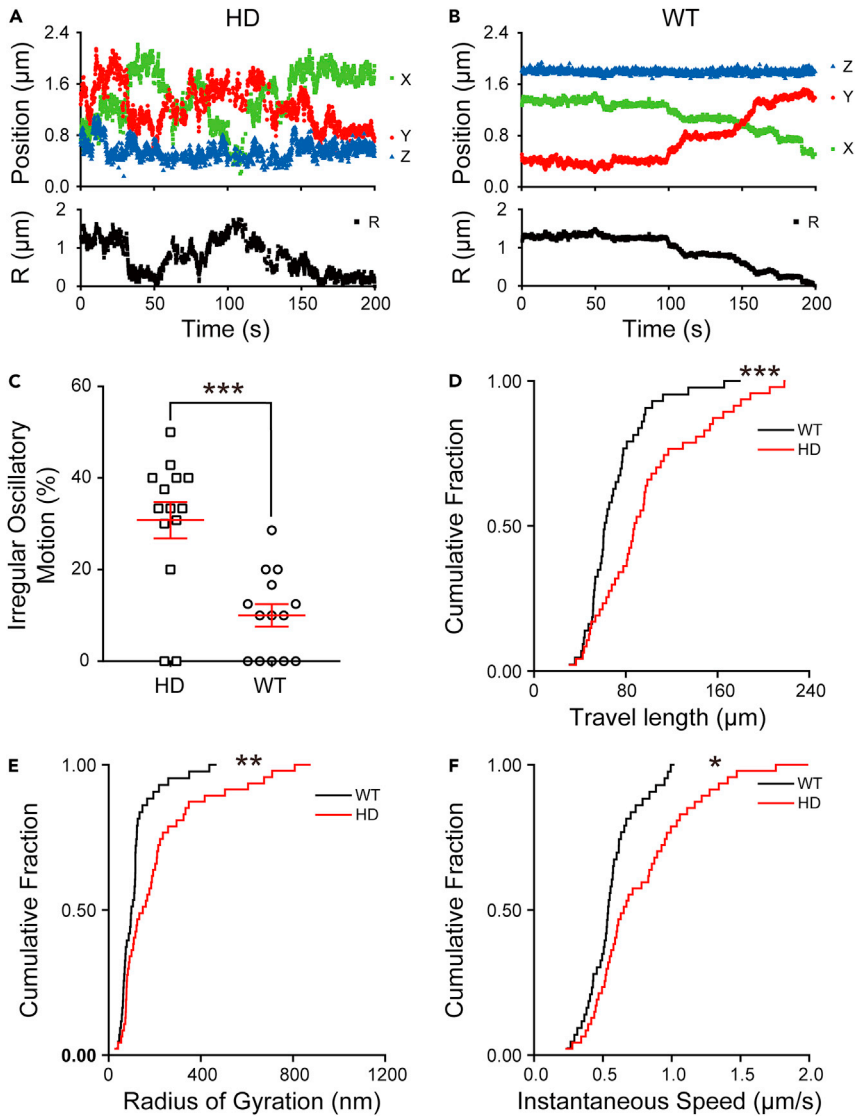

Figure 4. Non-releasing synaptic vesicles in HD neurons have abnormal irregular oscillatory motion

(A and B) Representative time courses of the three-dimensional position and radial distance (R) of a single non-releasing synaptic vesicle in an HD (A) and WT neuron (B).

(C) Summary of the percentage of synaptic vesicles with irregular oscillatory motion in HD (N = 14 experiments) and WT (N = 14) neurons. ***$p < 0.001$ (independent Student's *t*-test).

(D–F) Cumulative plots for travel length (D), radius of gyration (E), and instantaneous speed (F) of non-releasing synaptic vesicles in HD (n = 47 vesicles, N = 14 experiments) and WT (n = 43, N = 14) neurons. *$p < 0.05$, **$p < 0.01$, and ***$p < 0.001$ (K-S test).

has been implicated in several neurodegenerative diseases, including Parkinson's disease (Breda et al., 2015) and HD (Kiral et al., 2018). For example, reduced Rab11 activity was reported to impair the formation of synaptic vesicles from recycling endosomes in HD (Li et al., 2009a, 2009b). In addition, decreased Rab11 expression was reported in brain lysates obtained from R6/2 mice, a transgenic mouse model with strong phenotypic features associated with HD (Richards et al., 2011). Given the decreased expression and activity of Rab11 in HD, we hypothesized that the abnormal dynamics and vesicle pools of synaptic vesicles in HD neurons may be associated with a functional interaction between the mutant huntingtin protein and Rab11. In support of this hypothesis, we found that the overexpression of Rab11 rescued abnormal motion of releasing synaptic vesicles in HD neurons. Two-way ANOVA analyses indicated that overexpressed Rab11-GFP co-localized with QD-loaded synaptic vesicles (Figure 5A) significantly affected the net

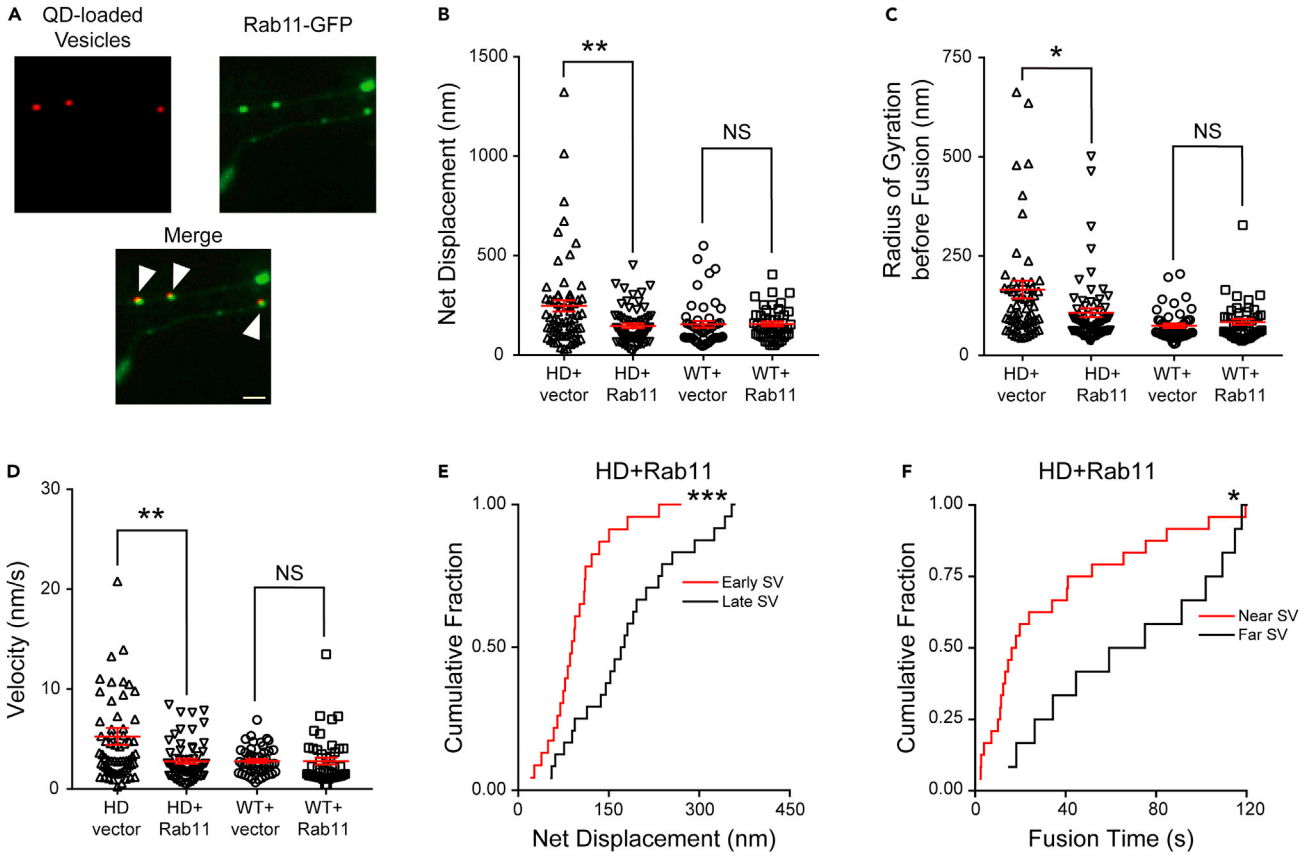

Figure 5. Overexpressing Rab11 rescues the abnormal dynamics and vesicle pools of releasing synaptic vesicles in HD neurons

(A) Representative images of QD-loaded vesicles (red) and Rab11-GFP (green) in HD neurons. Arrowheads indicate co-localization between QDs and Rab11-GFP. Scale bar: 2 μm.

(B–D) Summary of the net displacement (B), radius of gyration before fusion (C), and velocity (D) of releasing vesicles in HD and WT neurons transfected with an empty vector or a vector expressing Rab11-GFP. Overexpressing Rab11 reduced the net displacement (B), radius of gyration before fusion (C), and velocity (D) of releasing synaptic vesicles in HD neurons (empty vector, n = 64 vesicles, N = 14 experiments; Rab11, n = 62, N = 14) to the similar level as WT neurons. In contrast, overexpressing Rab11 did not affect the net displacement (B), radius of gyration (C), and velocity (D) of releasing synaptic vesicles in WT neurons (empty vector, n = 49 vesicles, N = 14 experiments; Rab11, n = 46, N = 13). *p < 0.05, **p < 0.01 and NS, not significant (Tukey's multiple comparisons test).

(E) Cumulative plots for the net displacement of early-releasing (n = 23 vesicles, N = 14 experiments) and late-releasing (n = 24, N = 14) synaptic vesicles in HD neurons overexpressing Rab11.

(F) Cumulative plots for fusion time of vesicles located near (n = 24 vesicles, N = 14 experiments) and far (n = 12, N = 14) from their fusion sites in HD neurons overexpressing Rab11. *p < 0.05, **p < 0.01, ***p < 0.001, and NS, not significant (K-S test).

displacement (p = 0.011), radius of gyration before fusion (p < 0.0001), and velocity (p = 0.022) of releasing synaptic vesicles in HD neurons. In particular, overexpressing Rab11-GFP significantly reduced the net displacement (p = 0.0010, Tukey's multiple comparisons test, Figure 5B), radius of gyration before fusion (p = 0.0237, Figure 5C), and velocity (p = 0.0011, Figure 5D) of releasing synaptic vesicles in HD neurons to the similar level as WT neurons. However, overexpressing Rab11 did not significantly alter these dynamic properties of releasing synaptic vesicles in WT neurons (Figures 5B–5D) (see also the results of Dunnett's multiple comparisons test in Table S1).

We also tested whether overexpressing Rab11 in HD neurons could rescue the abnormal relationship between the vesicle's release probability and its location. We found that early-releasing vesicles had significantly smaller net displacement compared with late-releasing vesicles in HD neurons containing overexpressed Rab11 (100 ± 11.4 nm (n = 23 vesicles, N = 14 experiments) vs. 186 ± 18.7 nm (n = 24, N = 14), respectively; p = 0.0008, K-S test) (Figure 5E), similar to our results in rat hippocampal neurons (Park et al., 2012) and our results in WT neurons shown in Figure 3B. In contrast, overexpressing Rab11 had no effect on net displacement of early-releasing and late-releasing synaptic vesicles in WT neurons (Figures

S8A and S8B). We also found that overexpressing Rab11 in HD neurons rescued the abnormal relationship between the vesicle's initial location and fusion time in HD neurons; specifically, synaptic vesicles located within 100 nm from their fusion sites had significantly shorter fusion time compared with vesicles located >200 nm from their fusion sites in HD neurons containing overexpressed Rab11 (35.1 $\pm$ 7.35 s (n = 24) vs. 72.9 $\pm$ 11.88 s (n = 12), respectively; p = 0.037, K-S test) (Figure 5F). In contrast, overexpressing Rab11 had no significant effect on the relationship between the vesicle's initial location and fusion time in WT neurons (Figures S8C and S8D). Interestingly, we found that overexpressing Rab11 did not significantly affect the abnormal irregular oscillatory motion (Figure S9A), net displacement (Figure S9B), and radius of gyration (Figure S9C) of non-releasing vesicles in HD neurons based on the two-way ANOVA test and Tukey's multiple comparisons test (see the results of statistical analyses in Table S3).

To determine whether the increasing activity of Rab11 can rescue the abnormal dynamics and vesicle pools of releasing synaptic vesicles in HD neurons, we overexpressed a constitutively active form of Rab11 (Rab11Q70L, Rab11-CA) (Li et al., 2009a, 2009b) and found that overexpressing constitutively active Rab11 rescued abnormal dynamics (Figures S10A and S10B, Tukey's multiple comparisons test) and vesicle pools (Figures S10C and S10D, K-S test) of releasing synaptic vesicles in HD neuorns but did not affect dynamics of non-releasing synaptic vesicles in HD neurons (Figures S10E and S10F, Tukey's multiple comparisons test) (see also the results of Dunnett's multiple comparisons test in Table S4). The overexpression of a dominant negative form of Rab11 (Rab11S25N, Rab11-DN) (Li et al., 2009a) increased the average net displacement and radius of gyration before fusion of releasing synaptic vesicles in WT neurons but differences were not statistically significant (Figure S11 and Table S5). Thus, these results indicate that increasing activity of Rab11 can rescue the abnormal dynamics and vesicle pool of releasing synaptic vesicles in HD neurons.

Stabilizing actin filaments rescues the abnormal dynamics of non-releasing synaptic vesicles in the presynaptic terminals of HD neurons

Previous studies showed that the huntingtin protein associates with actin filaments (Angeli et al., 2010; Tousley et al., 2019), possibly mediating transport of synaptic vesicles to presynaptic terminals. We therefore hypothesized that stabilizing actin filaments could rescue the abnormal motion of non-releasing vesicles in the presynaptic terminals of HD neurons. Consistent with this hypothesis, treating neurons with 5 μM jasplakinolide (JKL), which promotes actin polymerization and stabilizes actin filaments (Bae et al., 2012), significantly affected the irregular oscillatory motion (p = 0.0033, two-way ANOVA analyses), travel length (p = 0.0038), radius of gyration (p = 0.012), and instantaneous speed (p < 0.0001) of non-releasing synaptic vesicles in HD neurons. Particularly, treatment of jasplakinolide significantly reduced the irregular oscillatory motion (p = 0.0002, Tukey's multiple comparisons test, N = 14 experiments, Figure 6A), travel length (p = 0.0014, Figure 6B), radius of gyration (p = 0.0018, Figure 6C), and instantaneous speed (p < 0.0001, Figure 6D) of non-releasing synaptic vesicles in HD neurons. In contrast, treating WT neurons with jasplakinolide did not significantly change the irregular oscillatory motion (Figure 6A), travel length (Figure 6B), radius of gyration (Figure 6C), and instantaneous speed (Figure 6D) of non-releasing vesicles in WT neurons (see also the results of Dunnett's multiple comparisons test in Table S2). In contrast, jasplakinolide did not have any significant effect on the net displacement of releasing vesicles in HD neurons (Figure S12A) and failed to rescue the abnormal relationship between vesicles' location and their release probability (Figures S12B and S12C). Thus, jasplakinolide specifically affects the behavior of non-releasing vesicles, but does not affect releasing vesicles in HD neurons. In addition, treating WT neurons with latrunculin A (an actin polymerization inhibitor) increased the average radius of gyration and travel length of non-releasing synaptic vesicles in WT neurons but differences were not statistically significant (Figure S13 and Table S6). Taken together, these results indicate that stabilizing actin filaments can rescue the abnormal dynamics of non-releasing vesicles in the presynaptic terminals of HD neurons.

DISCUSSION

Although synaptic dysfunction has been suggested to play an important pathogenic role in HD (Chen et al., 2018; Li et al., 2003b; Sepers and Raymond, 2014; Yu et al., 2018), whether the motion and/or vesicle pools of synaptic vesicles is disrupted in HD—particularly with respect to the dynamics of single synaptic vesicles—has not been investigated. To address these questions, we tracked the real-time three-dimensional positions of single synaptic vesicles in HD cortical neurons and found the abnormal dynamics and vesicle pools of releasing synaptic vesicles in the presynaptic terminals of HD neurons. Moreover, we found that non-releasing synaptic vesicles in the presynaptic terminals of HD neurons have an abnormally high prevalence of irregular oscillatory motion, increasing their travel length and radius of gyration. Importantly, the

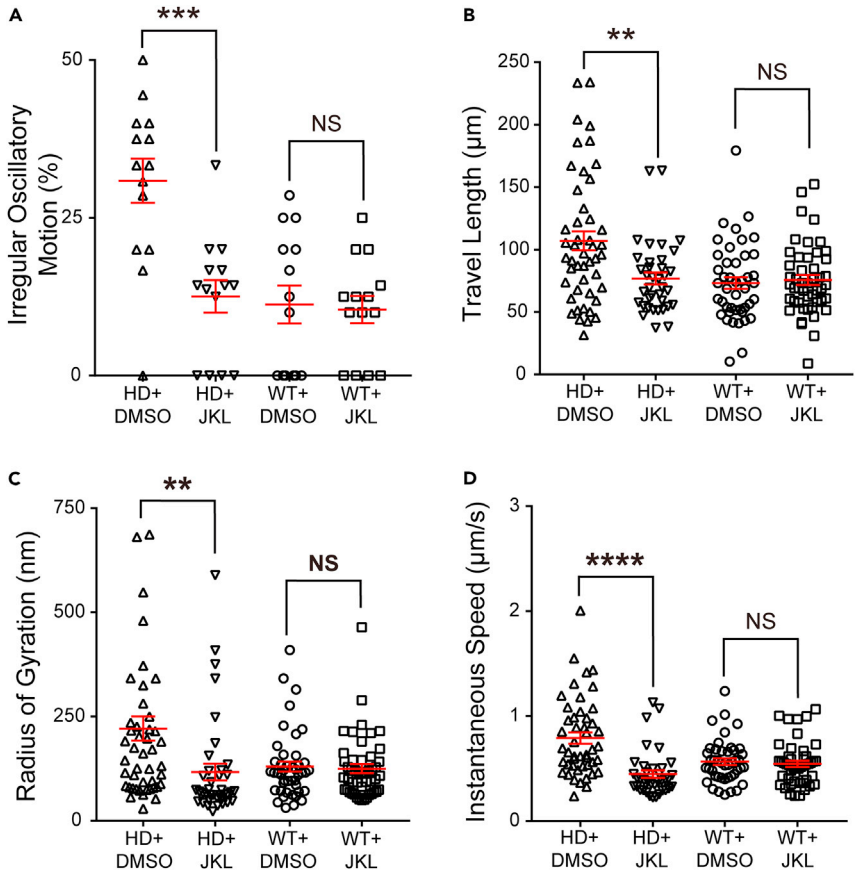

Figure 6. Stabilizing actin filaments rescues the abnormal motion of non-releasing synaptic vesicles in HD neurons

(A–D) Summary of abnormal irregular oscillatory motion (A), travel length (B), radius of gyration (C), and instantaneous speed (D) of non-releasing synaptic vesicles in WT and HD neurons treated with DMSO or 5 μM jasplakinolide (JKL). Treating with jasplakinolide reduced the percentage of irregular oscillatory motion (N = 14 experiments for every group) (A), travel length (B), radius of gyration (C), and instantaneous speed (D) of non-releasing synaptic vesicles in HD neurons (DMSO, n = 47 vesicles, N = 14 experiments; JKL, n = 37, N = 14) to the similar level as WT neurons. In contrast, jasplakinolide treatment did not affect the percentage of irregular oscillatory motion (A), travel length (B), radius of gyration (C), and instantaneous speed (D) in WT neurons (DMSO, n = 44 vesicles, N = 14 experiments; JKL, n = 48, N = 14). **p < 0.01, ***p < 0.001, ****p < 0.0001 and NS, not significant (Tukey's multiple comparisons test).

abnormal dynamics and vesicle pools of releasing synaptic vesicles and the abnormal motion of non-releasing vesicles in the presynaptic terminals of HD neurons were rescued by overexpressing Rab11 and stabilizing actin filaments with jasplakinolide, respectively.

The observed abnormal dynamics and vesicle pools of releasing synaptic vesicles of cultured neurons of HD mice at the single vesicle level suggest an alteration in neurotransmitter release in the presynaptic terminals of HD neurons, which is consistent with our previous findings of increased neurotransmitter release in single presynaptic terminals at an early age of zQ175 mice (Chen et al., 2018) and other HD models (Joshi et al., 2009; Romero et al., 2008) obtained from imaging and electrophysiology measurements. An alteration in synaptic vesicle release will contribute to impaired synaptic transmission in HD, as efficient synaptic transmission requires the accurate, reliable, and precisely timed release of neurotransmitters from synaptic vesicles. Thus, the observed abnormal dynamics and vesicle pools of single synaptic vesicles in HD neurons can lead to impaired synaptic transmission. In this respect, altered neurotransmitter release by the abnormal dynamics and vesicle pools of releasing synaptic vesicles may serve as an early pathogenic driver in HD (Milnerwood and Raymond, 2010).

Interestingly, we found that treating HD neurons with jasplakinolide (an actin filament stabilizer) rescued the abnormal motion of non-releasing vesicles in the presynaptic terminals, suggesting that the mutant

huntingtin protein may affect actin filaments (F-actin) in the presynaptic terminals. Our finding that jasplakinolide does not affect the vesicle pools of releasing synaptic vesicles suggests that F-actin alone does not play a role in separating early-releasing vesicles from late-releasing vesicles. On the other hand, we cannot rule out F-actin's other roles in the recycling of synaptic vesicles, particularly when a synaptic vesicle is internalized by "pinching off" from the presynaptic membrane in an endocytic pit (Wu et al., 2016). However, the increased irregular oscillatory motion in the presynaptic terminals of HD neurons likely reflects a possible defect in actin-based motility owing to altered actin dynamics by mutant huntingtin protein because mutant huntingtin protein was reported to alter the dynamics of actin filaments (Tousley et al., 2019) and myosin II and myosin V drive the movement of synaptic vesicles along actin filaments in the presynaptic terminals (Gramlich and Klyachko, 2017; Peng et al., 2012). Since myosin V was reported to tether synaptic vesicles at the plasma membrane (Maschi et al., 2018), we cannot rule out the possibility that the docking of synaptic vesicles will be affected in HD neurons.

We also found that overexpressing Rab11 or the constitutively active form of Rab11 rescued the abnormal motion of releasing synaptic vesicles. Interestingly, reduced Rab11 expression was previously reported in HD neurons (Richards et al., 2011), and overexpressing Rab11 in a *Drosophila* HD model rescued the neuronal phenotype (Steinert et al., 2012). Studies have also shown that the huntingtin protein facilitates the nucleotide exchange activity of Rab11, leading to Rab11 activation in cortical neurons (Li et al., 2008). In contrast, the mutant huntingtin protein has been shown to interfere with Rab11 activation, reducing endocytic vesicle formation in HD fibroblasts (Li et al., 2009b). Together, these findings suggest that the mutant huntingtin protein may downregulate or activate Rab11 to a lesser extent compared with the wild-type protein, leading to impaired vesicle dynamics in the presynaptic terminals of HD neurons. In this respect, it is interesting to note that overexpressing Rab11 or the constitutively active form of Rab11 rescue abnormal intermingling between early-releasing vesicles and late-releasing vesicles in HD neurons, suggesting that Rab11 may play an essential role in facilitating the localization of both early-releasing and late-releasing vesicles, and possibly non-releasing vesicles in the reserve pool. Nevertheless, further research is warranted to investigate the detailed mechanism by which Rab11 mediates the localization of synaptic vesicles based on release probability.

Although Rab11 overexpression and jasplakinolide treatment rescued the abnormal dynamics of single synaptic vesicles in the presynaptic terminals in our HD mouse model, we cannot rule out the possibility that other proteins and/or processes also contribute to abnormal vesicle dynamics in HD neurons. The huntingtin protein is a large scaffolding protein that interacts with several binding partners (Shirasaki et al., 2012), and disrupting these interactions can result in impaired glutamate release (Li et al., 2003a). Huntingtin-associated protein 1 (HAP1) is a major binding partner and has been shown to regulate the exocytosis of synaptic vesicles and play a role in the actin-based transport of insulin-containing granules in pancreatic beta cells (Mackenzie et al., 2016; Wang et al., 2015). Recently, Rab4, which coordinates vesicle trafficking, was reported to be affected in HD (White et al., 2020). Given that the huntingtin protein can interact with many proteins, some of which may have additional binding partners (Shirasaki et al., 2012), indirect interactions with the mutant huntingtin protein may contribute—at least in part—to the observed abnormal synaptic vesicle dynamics in HD neurons. Future research may therefore provide insight into the role that these associated proteins play with respect to the abnormal dynamics of synaptic vesicles in HD neurons.

Our findings in the early stage of HD are consistent with the disruption in the dynamics and recycling of synaptic vesicles reported in other neurodegenerative diseases, including Alzheimer's disease (Marsh and Alifragis, 2018) and Parkinson's disease (Hunn et al., 2015). Pathogenic tau binds to synaptic vesicles and disrupts synaptic vesicle's mobility and release (Zhou et al., 2017). Similarly, the aggregation of alpha-synuclein reduces the size of the recycling vesicle pool and impairs synaptic transmission (Nemani et al., 2010; Scott and Roy, 2012). These impairments in the synaptic vesicles dynamics and localization are likely mediated by cytoskeletal defects and Ras-associated small GTPases such as Rab11 (Breda et al., 2015; Udayar et al., 2013). Thus, overlap in the mechanisms that underlie different forms of neurodegeneration may be exploited when developing general therapies for neurodegenerative diseases.

In this study, we performed real-time three-dimensional tracking of single synaptic vesicles in cultured cortical neurons and found that synaptic vesicles in the presynaptic terminals of presymptomatic HD mice have the abnormal dynamics and vesicle pools of releasing synaptic vesicle, and abnormal irregular oscillatory motion of non-releasing synaptic vesicles. We also found that stabilizing actin filaments rescued the abnormal dynamics of non-releasing synaptic vesicles in the presynaptic terminals of HD neurons,

whereas overexpressing Rab11 rescued both the dynamics and vesicle pools of releasing vesicles in HD neurons. Together, these results suggest that the abnormal synaptic vesicle dynamics in the presynaptic terminals of HD neurons arise from the disrupted functions of actin filaments and Rab11, leading to impaired synaptic transmission in the early stage of HD. Thus, our results provide new insights into the role that synaptic vesicle dynamics play in the pathogenesis of HD and other neurodegenerative diseases.

Limitations of the study

In this study, we labeled single synaptic vesicles with QDs conjugated to biotinylated antibodies against the luminal domain of Syt1, which needs full-collapse fusion and thereafter endocytosis. Our results may not contain the features of synaptic vesicles which cannot uptake a QD during endocytosis. We showed that the abnormal dynamics and vesicle pools of releasing synaptic vesicles in HD neurons were rescued by overexpressing Rab11 and the abnormal irregular motion of non-releasing synaptic vesicles in HD neurons was rescued by applying jasplakinolide. However, we cannot rule out the existence of other rescue pathways, which have not been explored in the current study.

STAR★METHODS

Detailed methods are provided in the online version of this paper and include the following:

- KEY RESOURCES TABLE
- RESOURCE AVAILABILITY
  - Lead contact
  - Materials availability
  - Data and code availability
- EXPERIMENTAL MODEL AND SUBJECT DETAILS
  - Mouse strains
- METHODS DETAILS
  - Primary cortical cultured neurons
  - Three-dimensional tracking of single QD-loaded synaptic vesicles
  - Real-time imaging of single QD-labeled synaptic vesicles in cultured neurons
  - Overexpression of Rab11-GFP, EGFP-Rab11AQ70L and GFP-Rab11 DN
  - Jasplakinolide and latrunculin A treatment
- QUANTIFICATION AND STATISTICAL ANALYSIS

SUPPLEMENTAL INFORMATION

Supplemental information can be found online at https://doi.org/10.1016/j.isci.2021.103181.

ACKNOWLEDGMENTS

We thank Dr. Richard W. Tsien for generous support and helpful discussions, Dr. Sukho Lee for helpful discussions, and Dr. Curtis F. Barrett for critically reading the manuscript. This work was supported by grants from the Research Grants Council of Hong Kong (26101117, 16101518, N_HKUST613/17, and A-HKUST603/17 to H.P.), the Innovation and Technology Commission (ITCPD/17-9 to H.P.) and Joint Council Office (Grant No. BMSI/15-800003-SBIC-OOE to SJ).

AUTHOR CONTRIBUTIONS

S.C. and H.P. designed the experiments. S.C., H.Y., C.H.L., and C.P. performed the experiments. S.C., H.Y., C.H.L., C.P., and G.P. analyzed the data. S.C., L.Y.T., S.J., and H.P. wrote the manuscript. All authors read and approved the final manuscript.

DECLARATION OF INTERESTS

The authors declare no competing interests.

Received: May 12, 2021
Revised: August 30, 2021
Accepted: September 23, 2021
Published: October 22, 2021

REFERENCES

Alabi, A.A., and Tsien, R.W. (2012). Synaptic vesicle pools and dynamics. Cold Spring Harb. Perspect. Biol. *4*, a013680.

Alsina, A., Lai, W.M., Wong, W.K., Qin, X., Zhang, M., and Park, H. (2017). Real-time subpixel-accuracy tracking of single mitochondria in neurons reveals heterogeneous mitochondrial motion. Biochem. Biophys. Res. Commun. *493*, 776–782.

Angeli, S., Shao, J., and Diamond, M.I. (2010). F-actin binding regions on the androgen receptor and huntingtin increase aggregation and alter aggregate characteristics. PLoS One *5*, e9053.

Bae, J., Sung, B.H., Cho, I.H., and Song, W.K. (2012). F-actin-dependent regulation of NESH dynamics in rat hippocampal neurons. PLoS One *7*, e34514.

Benn, C.L., Sun, T., Sadri-Vakili, G., McFarland, K.N., DiRocco, D.P., Yohrling, G.J., Clark, T.W., Bouzou, B., and Cha, J.H. (2008). Huntingtin modulates transcription, occupies gene promoters in vivo, and binds directly to DNA in a polyglutamine-dependent manner. J. Neurosci. *28*, 10720–10733.

Breda, C., Nugent, M.L., Estranero, J.G., Kyriacou, C.P., Outeiro, T.F., Steinert, J.R., and Giorgini, F. (2015). Rab11 modulates α-synuclein-mediated defects in synaptic transmission and behaviour. Hum. Mol. Genet. *24*, 1077–1091.

Cepeda, C., and Levine, M.S. (2020). Synaptic dysfunction in huntington's disease: lessons from genetic animal models. Neuroscientist. https://doi.org/10.1177/1073858420972662.

Chen, S., Yu, C., Rong, L., Li, C.H., Qin, X., Ryu, H., and Park, H. (2018). Altered synaptic vesicle release and Ca(2+) influx at single presynaptic terminals of cortical neurons in a knock-in mouse model of huntington's disease. Front. Mol. Neurosci. *11*, 478.

Forte, L.A., Gramlich, M.W., and Klyachko, V.A. (2017). Activity-dependence of synaptic vesicle dynamics. J. Neurosci. *37*, 10597–10610.

Gramlich, M.W., and Klyachko, V.A. (2017). Actin/Myosin-V- and activity-dependent inter-synaptic vesicle exchange in central neurons. Cell Rep. *18*, 2096–2104.

Ho, L.W., Brown, R., Maxwell, M., Wyttenbach, A., and Rubinsztein, D.C. (2001). Wild type Huntingtin reduces the cellular toxicity of mutant Huntingtin in mammalian cell models of Huntington's disease. J. Med. Genet. *38*, 450–452.

Hunn, B.H., Cragg, S.J., Bolam, J.P., Spillantini, M.G., and Wade-Martins, R. (2015). Impaired intracellular trafficking defines early Parkinson's disease. Trends Neurosci. *38*, 178–188.

Jahn, R., and Fasshauer, D. (2012). Molecular machines governing exocytosis of synaptic vesicles. Nature *490*, 201–207.

Joshi, P.R., Wu, N.P., Andre, V.M., Cummings, D.M., Cepeda, C., Joyce, J.A., Carroll, J.B., Leavitt, B.R., Hayden, M.R., Levine, M.S., et al. (2009). Age-dependent alterations of corticostriatal activity in the YAC128 mouse model of Huntington disease. J. Neurosci. *29*, 2414–2427.

Kamin, D., Lauterbach, M.A., Westphal, V., Keller, J., Schonle, A., Hell, S.W., and Rizzoli, S.O. (2010). High- and low-mobility stages in the synaptic vesicle cycle. Biophys. J. *99*, 675–684.

Kiral, F.R., Kohrs, F.E., Jin, E.J., and Hiesinger, P.R. (2018). Rab GTPases and membrane trafficking in neurodegeneration. Curr. Biol. *28*, R471–r486.

Kokotos, A.C., Peltier, J., Davenport, E.C., Trost, M., and Cousin, M.A. (2018). Activity-dependent bulk endocytosis proteome reveals a key presynaptic role for the monomeric GTPase Rab11. Proc. Natl. Acad. Sci. U S A *115*, E10177–e10186.

Kyung, J.W., Kim, J.M., Lee, W., Ha, T.Y., Cha, S.H., Chung, K.H., Choi, D.J., Jou, I., Song, W.K., Joe, E.H., et al. (2018). DJ-1 deficiency impairs synaptic vesicle endocytosis and reavailability at nerve terminals. Proc. Natl. Acad. Sci. U S A *115*, 1629–1634.

Lee, S., Jung, K.J., Jung, H.S., and Chang, S. (2012). Dynamics of multiple trafficking behaviors of individual synaptic vesicles revealed by quantum-dot based presynaptic probe. PLoS One *7*, e38045.

Li, H., Wyman, T., Yu, Z.X., Li, S.H., and Li, X.J. (2003a). Abnormal association of mutant huntingtin with synaptic vesicles inhibits glutamate release. Hum. Mol. Genet. *12*, 2021–2030.

Li, J.Y., Plomann, M., and Brundin, P. (2003b). Huntington's disease: a synaptopathy? Trends Mol. Med. *9*, 414–420.

Li, X., Sapp, E., Chase, K., Comer-Tierney, L.A., Masso, N., Alexander, J., Reeves, P., Kegel, K.B., Valencia, A., Esteves, M., et al. (2009a). Disruption of Rab11 activity in a knock-in mouse model of Huntington's disease. Neurobiol. Dis. *36*, 374–383.

Li, X., Sapp, E., Valencia, A., Kegel, K.B., Qin, Z.H., Alexander, J., Masso, N., Reeves, P., Ritch, J.J., Zeitlin, S., et al. (2008). A function of huntingtin in guanine nucleotide exchange on Rab11. Neuroreport *19*, 1643–1647.

Li, X., Standley, C., Sapp, E., Valencia, A., Qin, Z.H., Kegel, K.B., Yoder, J., Comer-Tierney, L.A., Esteves, M., Chase, K., et al. (2009b). Mutant huntingtin impairs vesicle formation from recycling endosomes by interfering with Rab11 activity. Mol. Cell. Biol. *29*, 6106–6116.

Liu, G. (2003). Presynaptic control of quantal size: kinetic mechanisms and implications for synaptic transmission and plasticity. Curr. Opin. Neurobiol. *13*, 324–331.

MacDonald, M.E., Ambrose, C.M., Duyao, M.P., Myers, R.H., Lin, C., Srinidhi, L., Barnes, G., Taylor, S.A., Jame, M., Groot, N., et al. (1993). A novel gene containing a trinucleotide repeat that is expanded and unstable on Huntington's disease chromosomes. The Huntington's Disease Collaborative Research Group. Cell *72*, 971–983.

Mackenzie, K.D., Lumsden, A.L., Guo, F., Duffield, M.D., Chataway, T., Lim, Y., Zhou, X.F., and Keating, D.J. (2016). Huntingtin-associated protein-1 is a synapsin I-binding protein regulating synaptic vesicle exocytosis and synapsin I trafficking. J. Neurochem. *138*, 710–721.

Marsh, J., and Alifragis, P. (2018). Synaptic dysfunction in Alzheimer's disease: the effects of amyloid beta on synaptic vesicle dynamics as a novel target for therapeutic intervention. Neural Regen. Res. *13*, 616–623.

Maschi, D., Gramlich, M.W., and Klyachko, V.A. (2018). Myosin V functions as a vesicle tether at the plasma membrane to control neurotransmitter release in central synapses. Elife *7*, e39440.

Menalled, L.B., Kudwa, A.E., Miller, S., Fitzpatrick, J., Watson-Johnson, J., Keating, N., Ruiz, M., Mushlin, R., Alosio, W., McConnell, K., et al. (2012). Comprehensive behavioral and molecular characterization of a new knock-in mouse model of Huntington's disease: zQ175. PLoS One *7*, e49838.

Milnerwood, A.J., and Raymond, L.A. (2010). Early synaptic pathophysiology in neurodegeneration: insights from Huntington's disease. Trends Neurosci. *33*, 513–523.

Nemani, V.M., Lu, W., Berge, V., Nakamura, K., Onoa, B., Lee, M.K., Chaudhry, F.A., Nicoll, R.A., and Edwards, R.H. (2010). Increased expression of alpha-synuclein reduces neurotransmitter release by inhibiting synaptic vesicle reclustering after endocytosis. Neuron *65*, 66–79.

Park, C., Chen, X., Tian, C.L., Park, G.N., Chenouard, N., Lee, H., Yeo, X.Y., Jung, S., Tsien, R.W., Bi, G.Q., et al. (2021). Unique dynamics and exocytosis properties of GABAergic synaptic vesicles revealed by three-dimensional single vesicle tracking. Proc. Natl. Acad. Sci. U S A *118*, e2022133118.

Park, H., Li, Y., and Tsien, R.W. (2012). Influence of synaptic vesicle position on release probability and exocytotic fusion mode. Science *335*, 1362–1366.

Park, H., Toprak, E., and Selvin, P.R. (2007). Single-molecule fluorescence to study molecular motors. Q. Rev. Biophys. *40*, 87–111.

Peng, A., Rotman, Z., Deng, P.Y., and Klyachko, V.A. (2012). Differential motion dynamics of synaptic vesicles undergoing spontaneous and activity-evoked endocytosis. Neuron *73*, 1108–1115.

Qin, X., Tsien, R.W., and Park, H. (2019). Real-time three-dimensional tracking of single synaptic vesicles reveals that synaptic vesicles undergoing kiss-and-run fusion remain close to their original fusion site before reuse. Biochem. Biophys. Res. Commun. *514*, 1004–1008.

Richards, P., Didszun, C., Campesan, S., Simpson, A., Horley, B., Young, K.W., Glynn, P., Cain, K., Kyriacou, C.P., Giorgini, F., et al. (2011). Dendritic spine loss and neurodegeneration is rescued by Rab11 in models of Huntington's disease. Cell Death Differ. *18*, 191–200.

Rigamonti, D., Sipione, S., Goffredo, D., Zuccato, C., Fossale, E., and Cattaneo, E. (2001).

Huntingtin's neuroprotective activity occurs via inhibition of procaspase-9 processing. J. Biol. Chem. *276*, 14545–14548.

Romero, E., Cha, G.H., Verstreken, P., Ly, C.V., Hughes, R.E., Bellen, H.J., and Botas, J. (2008). Suppression of neurodegeneration and increased neurotransmission caused by expanded full-length huntingtin accumulating in the cytoplasm. Neuron *57*, 27–40.

Saudou, F., and Humbert, S. (2016). The biology of huntingtin. Neuron *89*, 910–926.

Schippling, S., Schneider, S.A., Bhatia, K.P., Munchau, A., Rothwell, J.C., Tabrizi, S.J., and Orth, M. (2009). Abnormal motor cortex excitability in preclinical and very early Huntington's disease. Biol. Psychiatry *65*, 959–965.

Schulte, J., and Littleton, J.T. (2011). The biological function of the Huntingtin protein and its relevance to Huntington's Disease pathology. Curr. Trends Neurol. *5*, 65–78.

Scott, D., and Roy, S. (2012). α-Synuclein inhibits intersynaptic vesicle mobility and maintains recycling-pool homeostasis. J. Neurosci. *32*, 10129–10135.

Sepers, M.D., and Raymond, L.A. (2014). Mechanisms of synaptic dysfunction and excitotoxicity in Huntington's disease. Drug Discov. Today *19*, 990–996.

Shirasaki, D.I., Greiner, E.R., Al-Ramahi, I., Gray, M., Boontheung, P., Geschwind, D.H., Botas, J., Coppola, G., Horvath, S., Loo, J.A., et al. (2012). Network organization of the huntingtin proteomic interactome in mammalian brain. Neuron *75*, 41–57.

Steinert, J.R., Campesan, S., Richards, P., Kyriacou, C.P., Forsythe, I.D., and Giorgini, F. (2012). Rab11 rescues synaptic dysfunction and behavioural deficits in a Drosophila model of Huntington's disease. Hum. Mol. Genet. *21*, 2912–2922.

Sudhof, T.C. (2004). The synaptic vesicle cycle. Annu. Rev. Neurosci. *27*, 509–547.

Sudhof, T.C., and Rizo, J. (2011). Synaptic vesicle exocytosis. Cold Spring Harb. Perspect. Biol. *3*, a005637.

Tao, C.L., Liu, Y.T., Sun, R., Zhang, B., Qi, L., Shivakoti, S., Tian, C.L., Zhang, P., Lau, P.M., Zhou, Z.H., et al. (2018). Differentiation and characterization of excitatory and inhibitory synapses by cryo-electron tomography and correlative microscopy. J. Neurosci. *38*, 1493–1510.

Tousley, A., Iuliano, M., Weisman, E., Sapp, E., Richardson, H., Vodicka, P., Alexander, J., Aronin, N., DiFiglia, M., and Kegel-Gleason, K.B. (2019). Huntingtin associates with the actin cytoskeleton and alpha-actinin isoforms to influence stimulus dependent morphology changes. PLoS One *14*, e0212337.

Udayar, V., Buggia-Prévot, V., Guerreiro, R.L., Siegel, G., Rambabu, N., Soohoo, A.L., Ponnusamy, M., Siegenthaler, B., Bali, J., Simons, M., et al. (2013). A paired RNAi and RabGAP overexpression screen identifies Rab11 as a regulator of β-amyloid production. Cell Rep. *5*, 1536–1551.

Ullrich, O., Reinsch, S., Urbé, S., Zerial, M., and Parton, R.G. (1996). Rab11 regulates recycling through the pericentriolar recycling endosome. J. Cell Biol. *135*, 913–924.

Vonsattel, J.P., and DiFiglia, M. (1998). Huntington disease. J. Neuropathol. Exp. Neurol. *57*, 369–384.

Wang, Z., Peng, T., Wu, H., He, J., and Li, H. (2015). HAP1 helps to regulate actin-based transport of insulin-containing granules in pancreatic β cells. Histochem. Cell Biol. *144*, 39–48.

Watanabe, T.M., Sato, T., Gonda, K., and Higuchi, H. (2007). Three-dimensional nanometry of vesicle transport in living cells using dual-focus imaging optics. Biochem. Biophys. Res. Commun. *359*, 1–7.

Westphal, V., Rizzoli, S.O., Lauterbach, M.A., Kamin, D., Jahn, R., and Hell, S.W. (2008). Video-rate far-field optical nanoscopy dissects synaptic vesicle movement. Science *320*, 246–249.

White, J.A., 2nd, Krzystek, T.J., Hoffmar-Glennon, H., Thant, C., Zimmerman, K., Iacobucci, G., Vail, J., Thurston, L., Rahman, S., and Gunawardena, S. (2020). Excess Rab4 rescues synaptic and behavioral dysfunction caused by defective HTT-Rab4 axonal transport in Huntington's disease. Acta Neuropathol. Commun. *8*, 97.

Wu, X.S., Lee, S.H., Sheng, J., Zhang, Z., Zhao, W.D., Wang, D., Jin, Y., Charnay, P., Ervasti, J.M., and Wu, L.G. (2016). Actin is crucial for all kinetically distinguishable forms of endocytosis at synapses. Neuron *92*, 1020–1035.

Yildiz, A., and Selvin, P.R. (2005). Fluorescence imaging with one nanometer accuracy: application to molecular motors. Acc. Chem. Res. *38*, 574–582.

Yu, C., Li, C.H., Chen, S., Yoo, H., Qin, X., and Park, H. (2018). Decreased BDNF release in cortical neurons of a knock-in mouse model of huntington's disease. Sci. Rep. *8*, 16976.

Yu, C., Zhang, M., Qin, X., Yang, X., and Park, H. (2016). Real-time imaging of single synaptic vesicles in live neurons. Front. Biol. *11*, 109–118.

Zhou, L., McInnes, J., Wierda, K., Holt, M., Herrmann, A.G., Jackson, R.J., Wang, Y.C., Swerts, J., Beyens, J., Miskiewicz, K., et al. (2017). Tau association with synaptic vesicles causes presynaptic dysfunction. Nat. Commun. *8*, 15295.

STAR★METHODS

KEY RESOURCES TABLE

REAGENT or RESOURCE	SOURCE	IDENTIFIER
Antibodies		
Rabbit polyclonal, biotinylated anti-Syt1	Synaptic Systems	105 103BT; RRID:AB_2619768
Chemicals, peptides, and recombinant proteins		
Hanks' Balanced Salt Solution	Gibco™	14175
Papain	Worthington	LS003127
DNAse	Sigma	D5025-375KU
Neurobasal Plus Medium	Gibco™	A3582901
Penicillin-Streptomycin	Gibco™	15070063
FBS	Gibco™	10270106
B27	Life technologies	17504001
Glutamax	Life technologies	35050061
poly-D-lysine	Sigma	P7405-5MG
FUDR	Sigma	U3003-5G
Qdot™ 625 Streptavidin Conjugate	Thermo Fisher Scientific	A10196
Lipofectamine 2000	Thermo Fisher Scientific	11668019
Jasplakinolide	Thermo Fisher Scientific	J7473
Latrunculin A	Thermo Fisher Scientific	L12370
Experimental models: Organisms/strains		
Mouse: B6J.zQ175 KI	The Jackson Laboratory	JAX stock #027410
Recombinant DNA		
GFP-Rab11 WT	Addgene	12674
EGFP-Rab11AQ70L	Addgene	49553
GFP-Rab11 DN	Addgene	12678
Software and algorithms		
Graphpad Prism 8	GraphPad Software, Inc	https://www.graphpad.com/scientific-software/prism/
Matlab 2018a	MathWorks	https://www.mathworks.com/products/matlab.html
MetaMorph	Molecular Devices	https://www.moleculardevices.com/products/cellular-imaging-systems/acquisition-and-analysis-software/metamorph-microscopy
IDL	Harris Geospatial Solutions, Inc.	https://www.l3harrisgeospatial.com/Software-Technology/IDL

RESOURCE AVAILABILITY

Lead contact

Further information and requests should be directed to and will be fulfilled by Hyokeun Park (hkpark@ust.hk).

Materials availability

This study did not generate new unique reagent.

Data and code availability

- All data reported in this paper will be shared by the lead contact upon request.

- The code used to process the raw video data and to generate the results included in the figures is available at: https://github.com/Park-Lab/Quantum-Dot-Vesicle-Dynamics-Project. Sample excel files containing matrix a and b were provided for testing our MATLAB programs.
- Any additional information required to reanalyze the data reported in this paper is available from the lead contact upon request.

EXPERIMENTAL MODEL AND SUBJECT DETAILS

Mouse strains

Mice of zQ175 (a Huntington's disease (HD) knock-in mouse model) were obtained from Jackson Laboratories and housed in the Animal and Plant Care Facility at the Hong Kong University of Science and Technology. Only heterozygous zQ175 mice were used for breeding. All procedures for mice handling were approved by Department of Health, Government of Hong Kong. All procedures were performed in accordance with approved protocols.

METHODS DETAILS

Primary cortical cultured neurons

Primary cortical neurons were prepared and cultured as described previously (Chen et al., 2018). Heterozygous zQ175 (HD) and WT neurons were collected from the cerebral cortex of postnatal day 0 (P0) heterozygous zQ175 pups and WT littermates. The dissected cortical neurons were digested briefly with papain (LS003127, Worthington Biochemical Corp., Lakewood, NJ, USA) and DNAse (D5025, Sigma-Aldrich). After gentle trituration, the density of neurons was determined, and neurons were plated on 12-mm glass coverslips precoated with poly-D-lysine (P7405, Sigma-Aldrich) in a 24-well plate as described previously (Chen et al., 2018). After 3 days *in vitro* (DIV3), 20 μM 5-fluoro-2′-deoxyuridine (F0503, Sigma-Aldrich) was added to the culture medium to inhibit proliferation of glial cells (Chen et al., 2018). Neurons were incubated at 37°C in humidified air containing 5% CO_2, and real-time imaging was performed at DIV14-17.

Three-dimensional tracking of single QD-loaded synaptic vesicles

Real-time imaging was performed similarly as described previously (Alsina et al., 2017; Chen et al., 2018) using an IX73 inverted microscope (Olympus) equipped with a 100x oil-immersion UPlanSAPO objective (Olympus) and a custom-built dual-focus imaging optics system containing a beamsplitter, a right angle mirror, lenses and mirrors (Park et al., 2012). Real-time three-dimensional tracking of QD-loaded vesicles was performed as follows. The real-time fluorescence images at two focus planes were captured side-by-side using an iXon Ultra EMCCD camera (Andor Technology Ltd., Belfast, UK) and a custom-made dual-focus imaging optics system. Custom programs written in IDL (Harris Geospatial Solutions, Inc.) were used to calculate the two-dimensional centroids and peak intensities of a QD at two different focal planes (I_1 and I_2) by fitting a two-dimensional Gaussian function to the fluorescence images. A PIFOC piezo stage (Physik Instrumente GmbH, Karlsruhe, Germany) was used to generate a calibration curve representing the relationship between the *z*-position and the relative difference in peak intensity$(I_1 - I_2)/(I_1 + I_2)$. The *z*-position was then calculated from the calibration curve using the corresponding value of $(I_1 - I_2)/(I_1 + I_2)$.

Real-time imaging of single QD-labeled synaptic vesicles in cultured neurons

Streptavidin-coated QDs (A10196, Thermo Fisher Scientific) were conjugated to biotinylated Syt1 antibodies (105 103BT, Synaptic Systems) by incubating at room temperature for one hour. The QD-conjugated antibodies were then added to a sample chamber containing a coverslip with attached neurons. Electrical field stimuli (1200 stimuli applied at 10 Hz for 120 s or 10 stimuli applied at 10 Hz for 1 s) were then applied in order to trigger the exocytosis and endocytosis of synaptic vesicles, causing the vesicles to take up antibodies-conjugated QDs; the stimuli were applied using a platinum parallel electrode connected to an SD9 Grass Stimulator (Grass Technologies). The Grass stimulator, beam shutter, and EMCCD camera were synchronized with a trigger from the camera using a Digidata 1550 interface (Molecular Devices), and Clampex (Molecular Devices) was used to generate the stimulation protocols. After stimulation and an additional 3-min incubation period, the chamber was rinsed extensively for 10 min with artificial cerebrospinal fluid (ACSF) containing (in mM): 120 NaCl, 4 KCl, 2 $CaCl_2$, 2 $MgCl_2$, 10 D-glucose, and 10 HEPES (300-310 mOsm, pH 7.2-7.4 with NaOH). Prior to capturing images, trypan blue was added to the ACSF at a final concentration of 2 μM. A 405 nm laser (Coherent Inc., USA) was used to excite QDs, and a dichroic

mirror (ZT405rdc, Chroma) and an emission filter (ET605/70m, Chroma) were used to capture the fluorescence signals. Real-time imaging experiments were performed at 10 Hz with an exposure time of 0.1 s for 200 s using the frame transfer mode of the EMCCD camera. After collecting a baseline of 20 s, 1200 electrical field stimuli (10 Hz for 120 s) were applied to the neurons, followed by an additional 60 s no stimulation.

Overexpression of Rab11-GFP, EGFP-Rab11AQ70L and GFP-Rab11 DN

To study any rescue effect of Rab11 on the dynamics of releasing synaptic vesicles, Lipofectamine 2000 (11668019, Thermo Fisher Scientific) was used to transfect cultured cortical neurons at DIV7 with each construct expressing either Rab11-GFP (plasmid #12674, Addgene), EGFP-Rab11AQ70L (constitutively active mutant of Rab11, plasmid #49553, Addgene)(Rab11-CA), GFP-Rab11 DN (plasmid #12678, Addgene) (Rab11-DN), or an empty vector. Transfected neurons were used for imaging experiments starting at DIV14. Imaging experiments were performed as described in the experimental method section for real-time imaging of single QD-labeled synaptic vesicles in this paper. Only QDs-labeled synaptic vesicles in transfected neurons were analyzed to examine any effect of Rab11.

Jasplakinolide and latrunculin A treatment

To study any rescue effect of jasplakinolide on the dynamics of non-releasing synaptic vesicles in HD neurons, jasplakinolide (5 μM; J7473, Thermo Fisher Scientific) or vehicle (DMSO) was added to the chamber after the addition of trypan blue to the extracellular solution. Imaging experiments were performed 10 min later as described in the experimental method section for real-time imaging of single QD-labeled synaptic vesicles in this paper. To study any effect of Latrunculin A on the dynamics of non-releasing synaptic vesicles, 0.1 μM Latrunculin A (L12370, Thermo Fisher Scientific) or vehicle (DMSO) was added to the chamber through perfusion system after trypan blue perfusion. After 3 min perfusion of Latrunculin A, imaging experiments were performed as described in the experimental method section for real-time imaging of single QD-labeled synaptic vesicles.

QUANTIFICATION AND STATISTICAL ANALYSIS

The fluorescence intensity within a given region of interest (ROI) was analyzed using MetaMorph software (Molecular Devices). Custom programs written in IDL (Harris Geospatial Solutions, Inc.) were used to calculate the peak intensities and two-dimensional centroids. The differences in the net displacement, travel length, fusion time, velocity, and radius of gyration of synaptic vesicles in HD and WT neurons were analyzed using the Kolmogorov–Smirnov test (GraphPad Prism 8). The differences in the fraction of synaptic vesicles with oscillatory motion were analyzed using an independent Student's *t*-test. The effects of Rab11, Rab11-CA and Rab11-DN overexpression, as well as jasplakinolide treatment, were analyzed using a two-way ANOVA (GraphPad Prism 8). Tukey's multiple comparisons test and Dunnett's multiple comparisons test were performed under two-way ANOVA test (GraphPad Prism 8). Differences were considered significant if $p < 0.05$. The Pearson's r, linear regression line of fusion time against net displacement of synaptic vesiclesin HD and WT neurons were calculated by OriginPro 9. The blinded analyses were performed for multiple groups.